
BEHAVIOR OF STEEL PLATE CONNECTIONS SUBJECT TO VARIOUS FIRE SCENARIOS

SERDAR SELAMET¹ and MARIA E. M. GARLOCK²

ABSTRACT

Shear connections connect a beam to a girder or to a column, and they are designed to resist only shear loads. In a fire event, the axial restraint provided by adjacent structure creates compressive and tensile forces in the beam and thus the connection. Using finite element (FE) models, this study examines single-plate shear connections that are bolted to the beam and welded to the supporting girder. The model is validated with experiments of bolted lap splice plates at elevated temperatures as well as full-scale experiments. A floor subassembly, i.e., the beam and girder and connection, is modeled so that appropriate forces (shear, axial, and moment) are applied to the connection. This floor subassembly is subject to a few fire scenarios to evaluate effects of rate of heating on the beam and connection components.

1. INTRODUCTION

Recent experimental research in the UK has shown that it is possible to design a steel beam without fire protection if tensile forces can develop in the connection at elevated temperatures^{1, 2, 3}. This same experimental research has shown that failure in the joint region may develop from tensile forces that arise from beam catenary action (where the beam hangs in tension) or beam contraction (during the cooling phase of the fire). Failure in the connection region is not a surprise since the connections are not designed to resist significant tensile forces at elevated temperatures.

Previous studies of steel frames under fire indicate that to get accurate predictions of the global response of a steel frame under fire, it is essential to understand how the connections perform. The connections essentially define the boundary conditions (restraint)

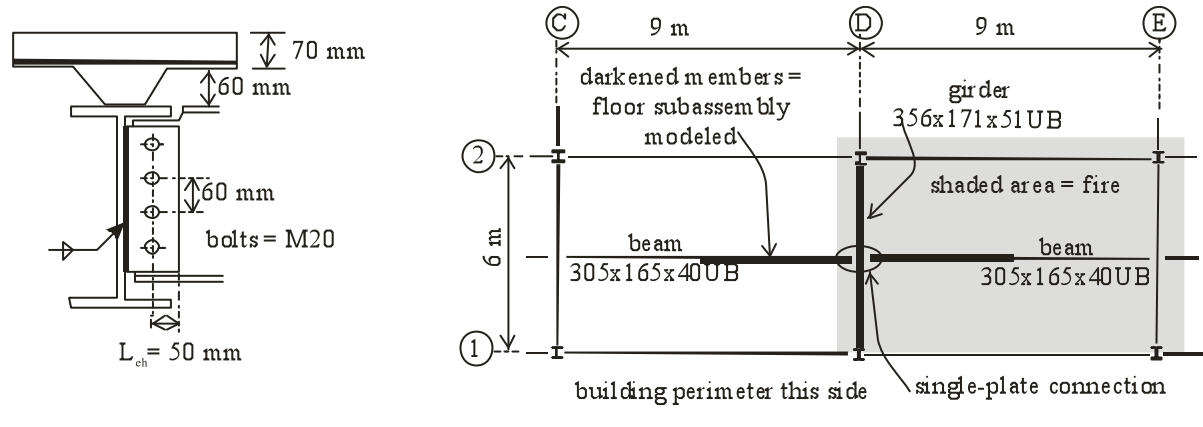
¹ Graduate Student, Princeton University, Dept. of Civil and Environmental Engineering, Princeton, NJ, 08544
email: sselamet@princeton.edu

² Assistant Professor, Princeton University, Dept. of Civil and Environmental Engineering, Princeton, NJ, 08544
email: mgarlock@princeton.edu

of the members, which in turn define the response of the steel frame. In a steel framed building, the connections support the floor beams and provide overall stability to the structure. In a fire scenario, the performance of the connections therefore plays a crucial role on the response of the structure as a whole.

Furthermore, a recent survey⁴ has shown that where partial floor collapse ensued in steel buildings under fire, that collapse always originated in the steel *shear* connections. Shear connections connect a beam to a girder or to a column, and they are designed to resist only shear loads. In a fire event, the axial restraint provided by adjacent structure creates compressive and tensile forces in the beam and thus the connection.

This paper presents some work that has recently begun at Princeton University on examining steel connections under fire. Specifically, *single-plate* (also called shear tab or fin plate) connections are presented in this paper (Figure 1). Using 3D finite element (FE) models, we examine single-plate shear connections that are bolted to the beam and welded to the supporting girder or column. This connection is studied as a part of a floor subassembly for reasons described below. The subassembly is subject to various fire scenarios to examine the effects of rate of heating on the beam and connection components.



single-plate connection detail

Building Plan

Figure 1. Structural design of the 2003 Cardington tests [Wald et al. 2006].

2. MODEL DESCRIPTION AND VALIDATION

2.1 Model Description

In a fire, the response of the beam, and hence the connection forces, are continually changing due to the thermal effects, the boundary conditions, and the large displacements that affect the mechanical response. The thermal effects produce changes in axial load and moment (if there is a thermal gradient) with time. It is therefore necessary to model the connections as a part of a floor subassembly that considers the interaction of the surrounding structure. The prototype for this floor subassembly and connection detail is the 2003 full scale test done in Cardington^{3, 5}. A compartment in an 8 story steel frame with concrete composite slab was tested under fire loads by BRE at the Cardington laboratory with the objective of examining the thermal and structural response of the slab, beams, columns and connections. A plan of the compartment that was tested and the corresponding beam sizes and connection details are shown in Figure 1.

Figure 2 shows the floor subassembly and connection finite element model. The slab is represented in the thermal analysis by not applying a fire load to the top flange. In the structural analysis, the lateral restraint provided by the slab is represented by fixing such

movement at the centerline nodes on the beam top flange. The slab vertical restraint (i.e., the flexural stiffness) is represented with elastic axial springs attached along the top flange of the beam. The stiffness of the springs was calibrated with experimental results. The flexible axial restraint provided to girder by column D1 is represented by springs with a stiffness based on Quiel and Garlock⁶. Symmetry boundary conditions are imposed on the beam ends (i.e., fixed horizontal translation at every node). The strength of the connection weld (Fig. 1) is not represented in the model; therefore it is assumed that this weld will not fail.

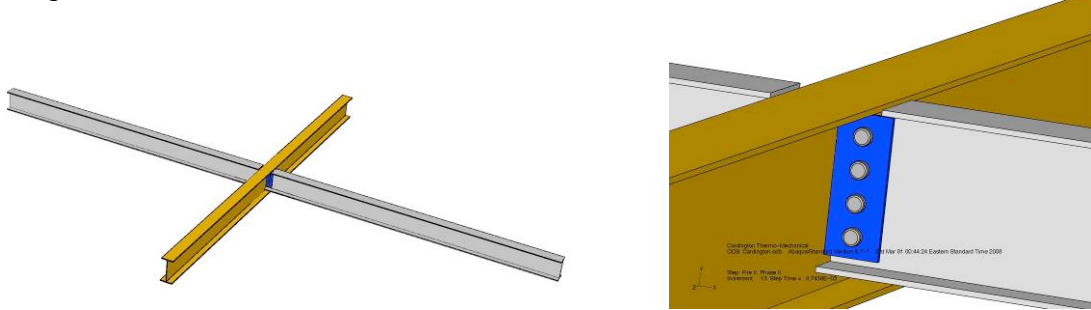


Figure 2. Finite element model of floor subassembly.

Commercially available ABAQUS/Standard is used to create the finite element models. 3D continuum stress eight node brick elements (C3D8) elements are used to represent the bolts and all steel plate elements. For the girder and two beams; C3D8 elements are used in proximity of contact areas and reduced integration elements (C3D8R) are used where no contact surfaces are defined and no local stress concentrations are expected. An uncoupled thermo-mechanical analysis is used on the subassembly where in the first phase (the thermal analysis) the heat transfer (Laplace equation) method is used to provide consistent transient nodal temperatures with respect to time. In the second phase (the mechanical analysis), the nodal temperatures are read from the thermal analysis and corresponding temperature dependent mechanical material properties are used.

The fire load imposed on the beam was related to thermocouple readings in the proximity of the beam region. For example, at midspan the beam had an imposed fire load that was slightly different from the beam at the connection region. The imposed fire load on the connection components (plates and bolts) were scaled down from that imposed on the beam so that the finite element thermal response matched closely to the results measured in the test (see Figure 3).

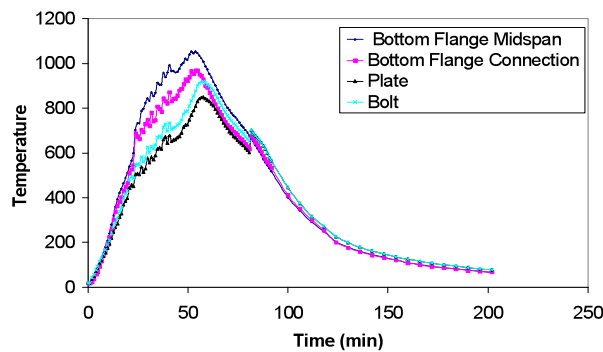


Figure 3. Applied fire loads to different parts of floor subassembly to represent heat sink effects as measured in the test.

The measured ambient yield stress of the beam (S275) and girder (S355) were 303 MPa (44 ksi) and 396 MPa (57 ksi), respectively. The bolts were grade 8.8 with a measured ultimate stress of 869 MPa (126 ksi)⁶. The connection plates were Grade 43 with a nominal yield and ultimate stress of 275 MPa (40 ksi) and 430 MPa (62 ksi). Eurocode reduction

factors were used to reduce the stress-strain material properties at high temperatures of plate, girder and beam members⁷. For the bolts, Kirby's suggested reduction factors are used⁸.

2.2 Validation: Lap Splice Experiments

Before constructing the floor subassembly with the connection details discussed above, we developed models of simple lap splices in order to (1) gain confidence using ABAQUS to represent connection details using smaller and simpler models; and (2) confirm that the ABAQUS models that we were building would be able to properly capture limit states such as bolt bearing and bolt shear. Our high temperature (steady-state) lap splice models were validated with experiments done by Yu⁹. Yu examined single bolt splice plate connections as well as double bolt. He tested these splices at ambient temperature and at varying levels of other temperatures up to 800° C. The specimens failed in a variety of manners including bearing, bolt shear, and block shear (in the case of the double bolts). Yu also examined the effects of varying the edge distance (L_{eh} in Figure 1) from 1 times to 1.5 times the bolt diameter (d_b).

Figure 4 shows the finite element ABAQUS model of the single bolt splice plate detail based on Yu. This figure shows how the finite element model can capture the limit states with reasonable accuracy. The finite element model was also able to capture the peak load reasonably well as shown in Table 1.

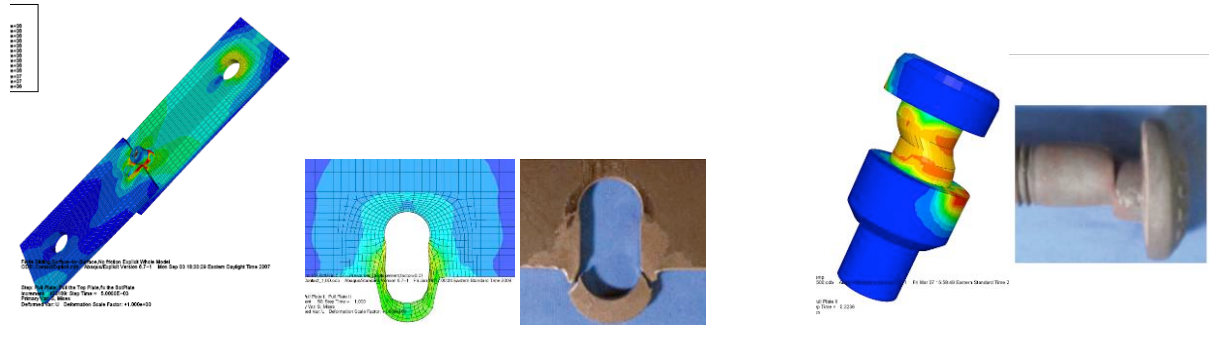


Figure 4. Finite element models of lap splices and photographs of experiments by Yu [2006] validating the results.

Table 1. Comparison of finite element results to Yu's experiments of a single splice plate connection with and $L_{eh} = 1.5d_b$. and $L_{eh} = 1.0d_b$.

Test	Temp(°C)	Maximum Load (kips)			Limit State	
		Experiment	Finite Element	Difference	Experiment	Finite Element
$L_{eh} = 1.5d_b$	20	41.8	38.5	8%	bearing	bearing
	100	42.8	36.3	15%	bearing	bearing
	500	23.6	21.1	10%	bolt shear	bolt shear
	700	6.0	6.1	2%	bolt shear	bolt shear
$L_{eh} = 1.0d_b$	20	25.6	24.2	5%	bearing	bearing
	100	27.9	22.7	19%	bearing	bearing
	500	20.2	17.4	14%	bearing	bearing
	700	5.5	5.3	5%	bolt shear	bearing

2.3 Validation - Full Building Experiment

The floor subassembly described in Section 2.1 was set up to represent as closely as possible BRE's multi-story full scale fire experiments performed at Cardington in 2003 as described previously. At the end of the experiment, the single-plate connection showed ovalization (plastic deformation) of the holes but no failure. The test also exhibited buckling of the beam lower flange as well as coped beam web near the connection. These experimental limit states are shown in the photograph of Figure 5. The finite element model captured these limit states as shown in Figure 6 and Figure 7. Experimental observations indicate that the beam lower flange buckling occurred during the early stages of fire, namely about 23 minutes into the heating phase. The Numerical model predicted lower flange buckling at 23.8 minutes, indicating a close match to the experiment.

Figure 8 shows the beam deflections at midspan. The difference in the vertical midspan deflection between the experiment and numerical model gets significantly larger once the beam web buckles at about 15 minutes into the heating phase. The numerical model fails to sustain the gravity load at about 27 minutes into the heating phase and fails by runaway. This behavior illustrates the importance of composite action and catenary effects of a slab on top of the steel frame. More sophisticated versions of the model will consider using 3D continuum elements to represent the slab.



Figure 5. Local buckling after 2003 Cardington experimental fire⁵.

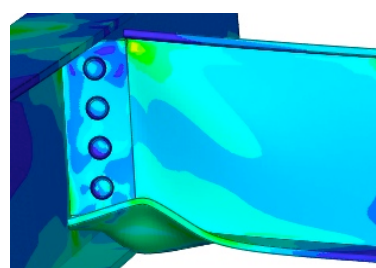


Figure 6. Finite element results showing flange local buckling.

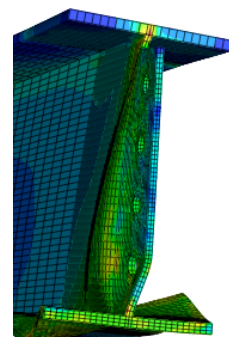


Figure 7. Finite element results showing beam web buckling.

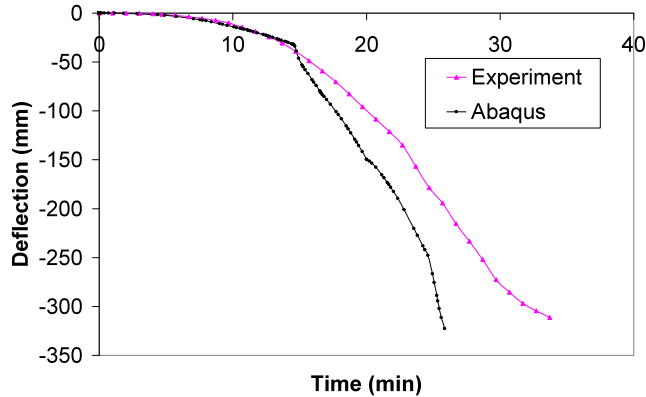


Figure 8. Vertical deflection at the beam midspan.

3. EFFECTS OF FIRE PARAMETERS

The parametric study described below uses the structural design, details, and loads of the 2003 Cardington experiments that were described previously. The differences between the parametric study and the Cardington test relate to the fire load and fire protection as follows: (1) the fire is assumed to be in the compartment bound by lines 1 and 2 and D and E and do not go beyond (see Figure 1); and (2) the girder on line D is assumed to have 15 mm thick fire protection on all fire exposed surfaces.

The reason for imposing these differences in the study is to force the limit states to develop on the beam and/or connection. Experimental observations of the Cardington test suggest that lateral-torsional buckling occurs at the girder ends during early stages of fire. Such global buckling would create convergence difficulties to the highly nonlinear (contact and geometric nonlinearity) static analysis.

Temperature recordings in Cardington compartment⁵ suggest that the predicted fire curve using Eurocode¹⁰ (i.e., “Cardington Design Fire Curve”) correctly predicted the duration of the burning period and the maximum temperature. However, it was not able to capture the fire growth rate within the compartment as seen in Figure 9. Furthermore, using the design fire curve, researchers predicted that local collapse would ensue. Hence one of the fire scenarios used in the parametric study was the recorded time-temperature history of the Cardington tests which is shown in Figure 9.

3.1 Fire Matrix

In the parametric study of different fires, the fire loads were scaled to the same ratio as that measured in the test (as described in Section 2.1 and Figure 3) to represent a cooler connection region due to heat sinks and a more realistic distribution of gas temperatures in the compartment. Figure 9 shows the first 2 hours of the different fire scenarios used in the study where the temperatures shown represent the temperature on beam midspan region. The parameters that were used to develop each parametric fire are described in Table 2. The time-temperature relationship is derived based on Eurocode provisions.¹⁰

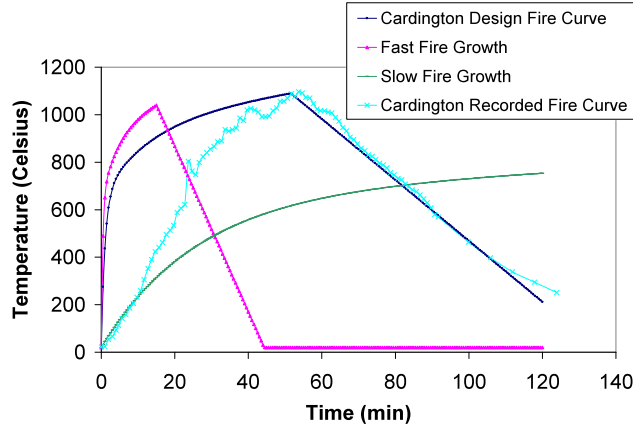


Figure 9. Several Fire Scenarios based on Cardington Compartment

The “Cardington Design” fire curve is a ventilation controlled fire that reaches a maximum temperature 1088 °C in about 52 minutes. The “Fast Fire Growth” parametric curve is created by taking the same compartment dimensions but using a larger opening factor, increasing the thermal inertia of surrounding materials for more heat absorption within the compartment and having a slightly smaller fire load density. This leads to a much faster fire growth reaching max temperature 1039 °C in about 15 minutes. This fire curve is severe but it is still within the limit of ventilation controlled fire category. The duration of heating gets smaller compared to the “Cardington Design” fire curve”; but the maximum temperature reached within the compartment stays relatively same. The decay rate of “Fast Fire Growth” fire curve is faster than “Cardington Design” fire curve.

The “Slow Fire Growth” parametric curve is created by taking a much higher fire load density combined with very small opening factor while taking the thermal inertia of surrounding materials about the same as in “Fast Fire Growth” fire curve. This leads to a relatively slow fire growth rate with reached temperature of 839 °C in 4 hours. The decay period would begin after 7 hours, if the fire lasts that long.

Table 2. Summary of Fire Curve Characteristics

Fire	Thermal Inertia (J/m ² *s ^{.5} K)	Energy Density Per floor area (MJ/m ²)	Opening Factor	T _{max} (°C)
Cardington Design	720	720	0.043	1088
Fast Fire Growth	1205	540	0.11	1039
Slow Fire Growth	1135	800	0.013	839

3.2 Results

Figures 10a and 10b show the axial force in the beam (P) versus the time of the fire at the midspan and at the connection region, respectively. As expected, a larger fire growth rate leads to a larger P growth rate and the axial force is essentially the same at both locations.

Figures 11a and 11b also show the axial force in the beam at both midspan and at the connection regions. This time however, P is plotted against the average beam temperature. One interesting result is that the slow fire growth scenario produces larger P. Since in a slow growing fire the temperature in the section will be more uniform through its depth, the thermal elongation is mostly taken out by axial elongation as opposed to curvature, which develops with thermal gradients.

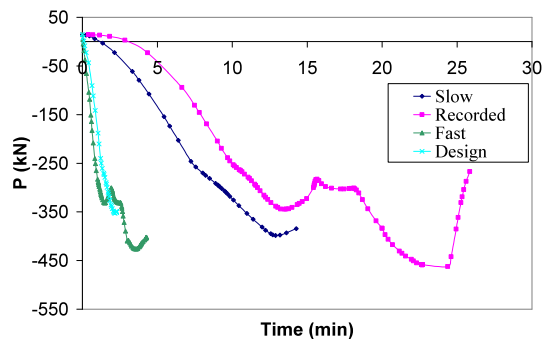


Figure 10(a). P vs. time at beam midspan.

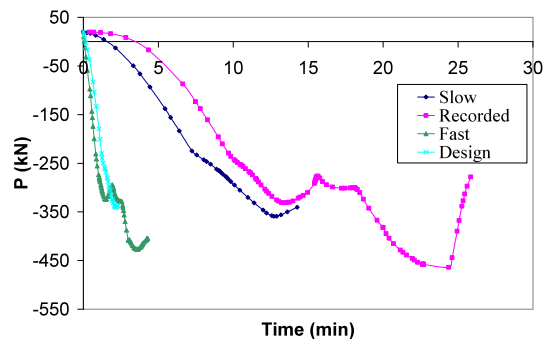


Figure 10(b). P vs. time near connection.

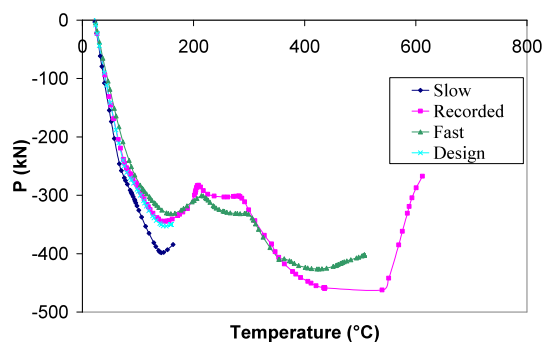


Figure 11(a). P vs. avg. beam temperature at midspan

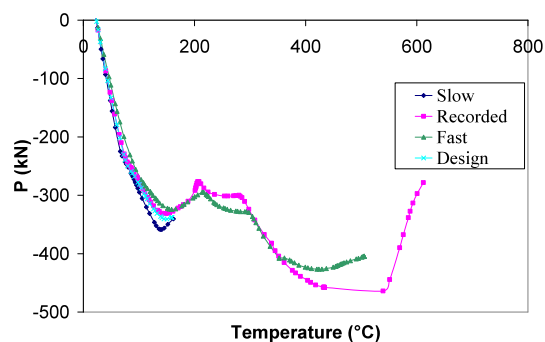


Figure 11(b). P vs. average beam temperature near connection.

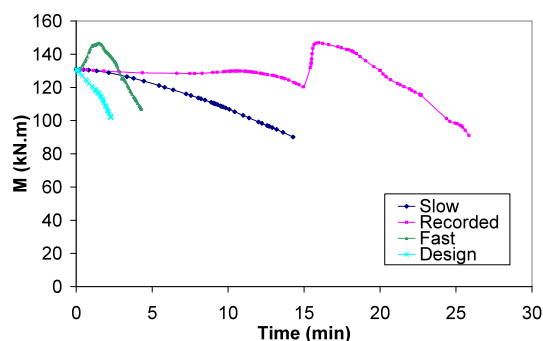


Figure 12(a). M vs. time at midspan

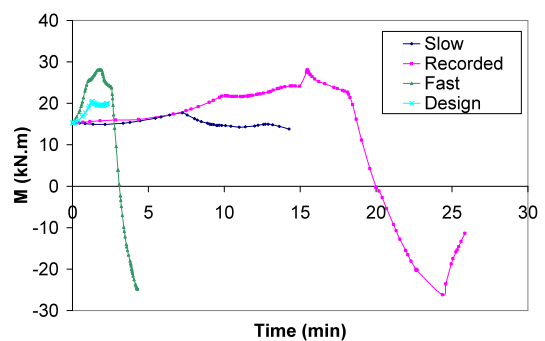


Figure 12(b). M vs. time near connection.

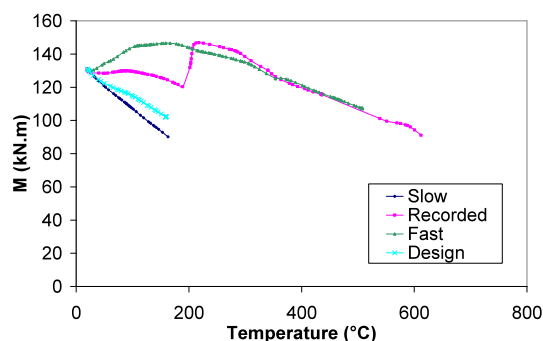


Figure 13(a). M vs. avg. beam temperature at midspan

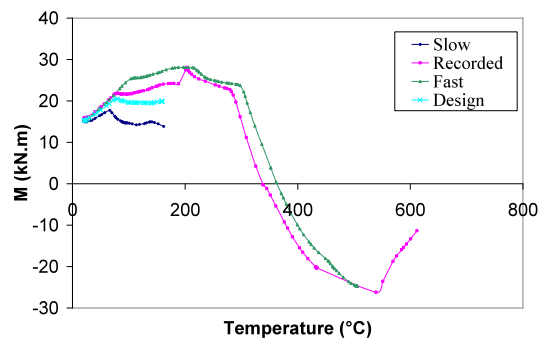


Figure 13(b). M vs. average beam temperature near connection.

Figure 12 and 13 plot the moment in the beam both at the connection region and at the midspan. We observe that the rate of heating has an effect on the moments that develop in the beam. This is due to the thermal gradients that are produced. In the fires that were able to reach elevated temperatures (recorded and fast fires), the moments in the connection region reversed direction (become negative) as seen in Figures 12(b) and 13(b). This is due to both the thermal gradients as well as the partial restraint provided by the connection (i.e., it is not an ideal pin connection). This negative moment develops as the deflections at beam midspan become large as seen in Figure 14.

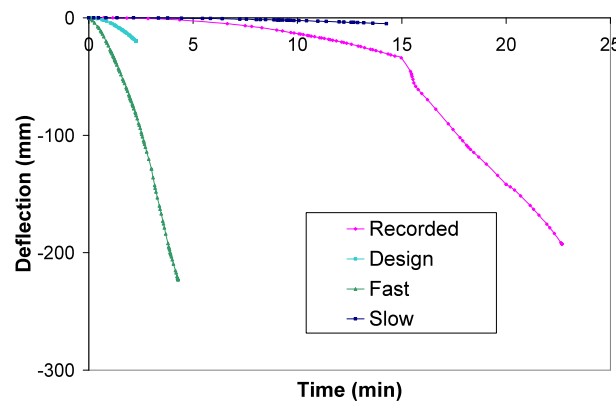


Figure 14. Vertical Deflections at Midspan.

Table 3 summarizes the parametric study results. For all parametric fires, beam web buckling is observed in the early stages of the fire due to the weak resistance of the coped beam web to the high temperature induced axial forces. However, the time and average beam temperature at which it is reached changes considerably as seen in Table 3.

While in the actual Cardington test local buckling of the beam lower flange is observed (as seen in Figures 5 and 8), only the “Fast Fire Growth” analysis reached this limit state. It is possible that when the numerical instabilities are overcome, the other analyses will also reach this limit state. Based on the automatic stabilization techniques employed by ABAQUS, we suspect that the other analyses terminated due to lateral torsional buckling near the beam support. This type of global buckling is observed in the Cardington test in the unprotected girder⁵, which is restrained in the axial direction by columns.

Table 3. Summary of Parametric Study Results

Test	Web buckling	Lower flange buckling	Analysis End	
			time (min)	temperature (°C)
Cardington Recorded	Yes (13 min)	No	23	436
Cardington Design	Yes (2.1min)	No	2.3	159
Fast Fire Growth	Yes (3.0 min)	Yes (4.2 min)	4.3	507
Slow Fire Growth	Yes (12.6 min)	No	14.3	163

4. SUMMARY AND CONCLUSION

A finite element model of a single plate shear connection was developed and validated against extensive experimental data. The model is successfully capable of predicting the limit states of bolt bearing, bolt shearing, flange local buckling, and the peak loads. This validation was performed against simple splice plate connection tests as well as a full-scale building test done at Cardington.

A parametric study was then performed to examine the effects of different fire characteristics. Since at the time of submission of this paper the analyses ended before the peak temperatures were reached, this study evaluated only the effect of heating rate. In all cases web buckling developed first due to the large compressive forces on the web and the lack of restraint due to the coping detail. The local instabilities occur during the very early stages of fire while most of the beam remains in elastic region.

A slow heating rate also produces higher axial compressive forces in the connection since there will be less thermal gradients and therefore less curvature to take out the thermal expansion of the beam. While the rate of heating does not affect the axial forces, it does affect the moments that develop in the connection region and therefore connection.

The rate of heating and the compressive connection forces that develop do not have a significant effect on the connection response as designed in this study. It does however have an effect on the beam response. It is expected that the effects of peak temperature and decay rate will have more of an impact on the connection performance.

Current research by the authors is not only developing modeling strategies to overcome numerical instabilities, but also looking at alternative means of representing the slab, which will play a crucial role during beam runaway. Future research will also examine the strength of welds in such connection details.

5. ACKNOWLEDGEMENTS

The authors are grateful to Professor Panos Papadopoulos (Dept. of Mechanical Engineering, University of California at Berkeley) for his assistance with ABAQUS and developing the finite element model.

6. REFERENCES

- [1] Wang, Y. and Ding, J. "Experimental Behaviour of Steel Joints to Concrete Filled Steel Tubular Columns in Fire," Proceedings of Fourth International Symposium on Steel Structures, Seoul, Korea, 16-18 November 2006.
- [2] Bailey, C.G., Lennon, T., and Moore, D.B., "The behavior of full-scale steel-framed buildings subjected to compartment fires," The Structural Engineer, Vol. 77, No. 8, pp. 15-21, 1999.
- [3] Lennon,T., and Moore, D. (2004). Client Report :Results and observations from full-scale fire test at BRE Cardington, 16 January 2003 Client report number 215-741.

- [4] Beitel, J., and Iwankiw, N. "Analysis of needs and existing capabilities for full-scale fire resistance testing." National Institute of Standards and Technology: NIST GCR 02-843. 1-86, 2002.
- [5] Wald, F., Simões da Silva, L., Moore, D.B., Lennon, T., Chadná, M., Santiago, A., Benes, M. and borges, L. "Experimental Behaviour of Steel Structures under Natural Fire", *Fire Safety Journal* 41 (7), pp. 509-522, 2006.
- [6] Garlock, M.E.M. and Quiel, S.E. (2008). "A Closed-Form Analysis of Perimeter Member Behavior in a Steel Building Frame Subject to Fire" (submitted for publication in *Engineering Structures*).
- [7] Eurocode 3: Design of steel structures – Part 1.2: General Rules – Structural fire design./ ENV 1993-1-2:2001/. European Committee for Standardization, Brussels, Belgium, 2001.
- [8] Kirby, B.R. "The Behavior of High-strength Grade 8.8 Bolts in Fire", *Journal of Constructional Steel Research*, Vol 33, p.3-38, 1995.
- [9] Yu, L. Behavior of Bolted Connection during and after a Fire, Ph.D. Dissertation, University of Texas at Austin, August 2006.
- [10] Eurocode 1: Actions on structures – Part 1-2: General actions – Actions on structures exposed to fire. EN 1991-1-2:2002. European Committee for Standardization, Brussels, Belgium, 2002.